COVER SHEET

Title : **Nonlinear Dynamic Behaviour of Impact Damage in a Composite Skin-Stiffener Structure**

Authors : T.H. Ooijevaar[1,3], M.D. Rogge[2], R. Loendersloot[3], L. Warnet[1], R. Akkerman[1] and A. de Boer[3]

[1] University of Twente,
Faculty of Engineering Technology,
Production Technology
P.O. Box 217, 7500AE, Enschede, The Netherlands

[2] NASA Langley Research Center,
Nondestructive Evaluationb Sciences Branch,
Mail Stop 231, 3B East Taylor Street, Hampton, VA, USA

[3] University of Twente,
Faculty of Engineering Technology, Dynamics Based Maintenance,
P.O. Box 217, 7500AE, Enschede, The Netherlands

Submitted to : 9th International Workshop on Structural Health Monitoring 2013

Corresponding author : T.H. Ooijevaar

University of Twente,
Faculty of Engineering Technology,
P.O. Box 217, 7500AE, Enschede, The Netherlands
E-mail: t.h.ooijevaar@utwente.nl

Abstract

One of the key issues in composite structures for aircraft applications is the early identification of damage. Often, service induced damage does not involve visible plastic deformation, but internal matrix related damage, like delaminations. A wide range of technologies, comprising global vibration and local wave propagation methods can be employed for health monitoring purposes. Traditional low frequency modal analysis based methods are linear methods. The effectiveness of these methods is often limited since they rely on a stationary and linear approximation of the system. The nonlinear interaction between a low frequency wave field and a local impact induced skin-stiffener failure is experimentally demonstrated in this paper. The different mechanisms that are responsible for the nonlinearities (opening, closing and contact) of the distorted harmonic waveforms are separated with the help of phase portraits. A basic analytical model is employed to support the observations.

T.H. Ooijevaar, L. Warnet and R. Akkerman, University of Twente, Faculty of Engineering Technology, Production Technology, P.O. Box 217, 7500AE Enschede, The Netherands

M.D. Rogge, NASA Langley Research Center, Nondestructive Evaluation Sciences Branch, Mail Stop 231, 3B East Taylor Street, Hampton, VA, USA

R. Loendersloot and A. de Boer, University of Twente, Faculty of Engineering Technology, Dynamics Based Maintenance, P.O. Box 217, 7500AE Enschede, The Netherands

1 Introduction

Composite skin-stiffener structures a typical aerospace structural component used to increase the bending stiffness of a component without a severe weight penalty [1]. Small defects at the skin-stiffener connection, caused by for example impact, can significantly affect the performance of such a component. Often, the damage does not involve visible plastic deformations, but is barely visible and internal matrix related, requiring a nondestructive damage evaluation technique to identify this damage.

A wide range of technologies can be employed to monitor the integrity of structural components [2–6]. Damage sensitive features are extracted in traditional low frequency modal analysis based damage identification methods by fitting a mathematical model to the responses measured [7]. The effectiveness of these methods is often limited since they rely on a stationary and linear approximation of the system. A more realistic damage description requires a physical understanding of the dynamic damage behavior. The interaction between damage and an acoustic wave field can yield dynamic mechanisms that exhibit complicated (material and geometrical) nonlinear behavior [8].

This paper addresses the analysis of the nonlinear dynamic behavior of impact induced damage in a composite skin-stiffener structure. The impact induced damage is located at the connection between the skin and the stiffener. The objective is to gain an understanding of the interaction between a dynamic wave field and the local skin-stiffener failure. An analytical model is utilized to support the interpretation of the results obtained. The experimental and analytical study presented in this paper contribute to the understanding of the nonlinear damage behavior in composite skin-stiffener structures. Hence, it helps the selection of suitable damage identification methodologies and supports the development of new health monitoring approaches.

2 Composite skin-stiffener structure

The structure investigated in this research is a thermoplastic skin-stiffener structure, as depicted in Figure 1. The butt-joint concept, developed by Fokker Aerostructures [1] is employed: the skin and stiffener are connected via an injection moulded filler and co-consolidated in the final manufacturing step. Both the skin and the stiffener are built from 16 individual plies of unidirectional carbon AS4D fibre reinforced thermoplastic (PEKK) material with a $[0/90]_{4,S}$ layup. The filler is made from PEKK and contains 20% short carbon fibres.

The damage scenario analyzed is a delamination between skin and stiffener: the most critical, but also a likely spot for a delamination to occur. Damage was introduced by utilizing a falling weight impact device and applying a repeated impact up to 15J. The ultrasonic C-scan in Figure 2 reveals a delamination at the interface between the skin and stiffener accompanied by a limited amount of failure between the first and second ply of the skin. Local delaminations were also introduced underneath one of the supports that was used during the impact testing.

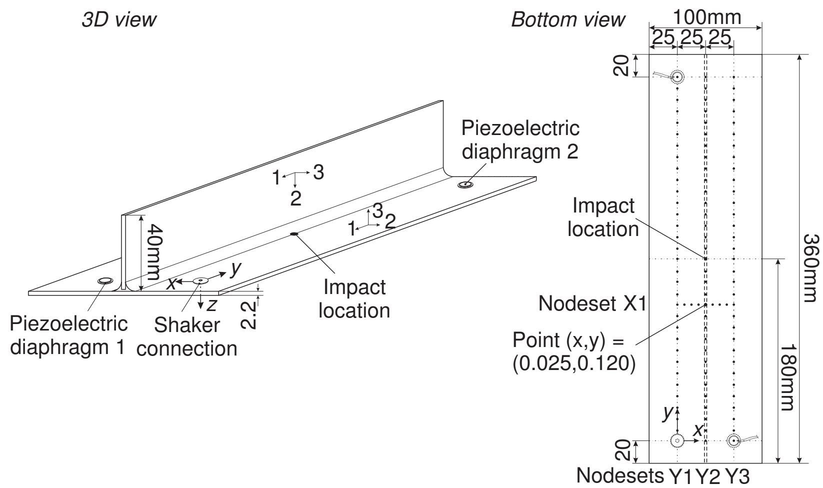

Figure 1: Three dimensional and bottom view of the composite skin-stiffener structure with a butt-joint stiffener. The dimensions, the measurement points (dots) and the impact location are indicated.

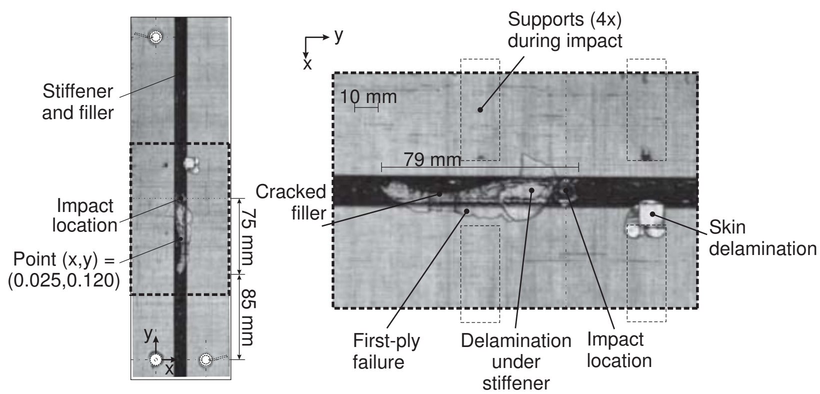

Figure 2: Ultrasonic C-scan of the impact damaged skin-stiffener structure, showing a complex combination of failure mechanisms near the skin-stiffener interface.

3 Experimental work

The set-up and data acquisition systems used for all experiments are schematically illustrated in Figure 3. The structure is freely suspended and the excitation is done with an electro-mechanical shaker. A laser vibrometer, mounted on an x/y traverse system, measured the velocities at different points at the skin of the structure (see Figure 1), both before and after the impact damage was introduced.

As a first step, the overall dynamic behavior of the structure is determined in terms of the natural frequencies and operational deflection shapes (ODS). An excitation signal composed of a linear sweep between 150 and 3050Hz was sent to the shaker. The time signals from the 51 (3×17) measuring points are converted to auto- and cross-power spectral densities $S_{F_iF_i}(\omega)$ and $S_{F_iv_j}(\omega)$. The mobility frequency response functions $H_{F_iv_j}(\omega)$ between the fixed excitation point i and the

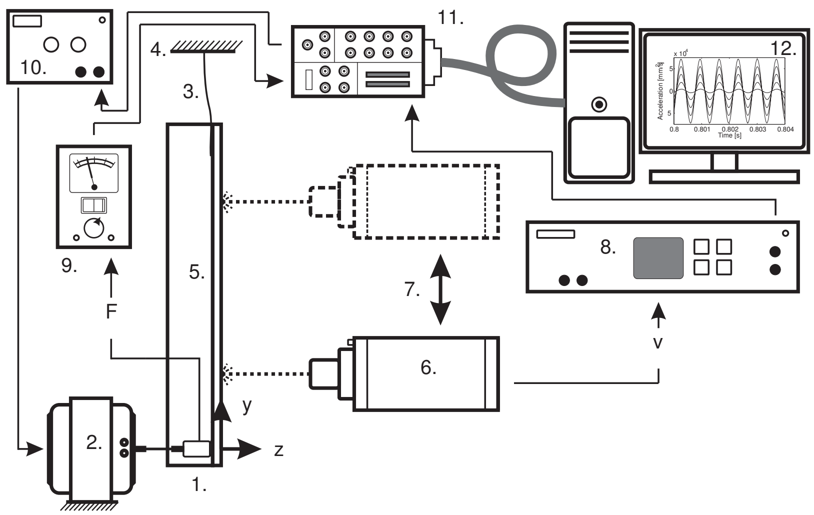

	Description	Hardware		Description	Hardware
1	Force transducer	PCB 208C02	7	Traverse system *x* / *y*	
2	Shaker	B&K 4809	8	Laser Vibrometer: controller	Polytec OFV 5000
3	Wired suspension		9	Condition amplifier	PCB Model 480D06
4	Fixed frame		10	Power amplifier	Dynakit Mark III 60W (2x)
5	Composite skin-stiffener structure		11	Data acquisition	NI PCI-6110E
6	Laser Vibrometer: sensor head	Polytec OFV-505	12	Computer with Labview Data Acquisition software	

Figure 3: Experimental set-up

roving measurement points j are subsequently calculated, according to:

$$H_{F_iV_j} = \frac{S_{F_iv_j}}{S_{F_iF_i}} \tag{1}$$

Figure 4 shows the magnitude of the total set of frequency response functions (FRFs) of the pristine structure. The operational deflection shapes of the structure are extracted at the natural frequencies – the sharp peaks in the FRF – with the help of peak picking. At these frequencies, the complex operational deflection shapes become predominantly real valued and are a close approximation of the associated mode shape. The 4th and 6th bending modes revealed to be of particular interest. The associated frequencies are $f_4 = 1456$Hz and $f_6 = 2328$Hz for the pristine and $\tilde{f}_4 = 1455$Hz and $\tilde{f}_6 = 2340$ for the damaged structure. The 6th natural frequency of the damage structure is unexpectedly higher than that of the pristine structure, which is caused by a shaker replacement, resulting in an increase of some of the natural frequencies. The type of deflection shape remained unchanged.

In the second step, the interaction between the damage and the dynamic deformation of the structure is studied by applying a single tone harmonic excitation signal. This signal corresponds to one of the natural frequencies, obtained in the overall dynamic analysis and is varied in strength. Only the steady state response is utilized because it is independent of the initial conditions. A period of 0.8 seconds was revealed to be sufficiently long for the transient (start-up) responses to become negligible. The settings for both measurements are gathered in Table 1.

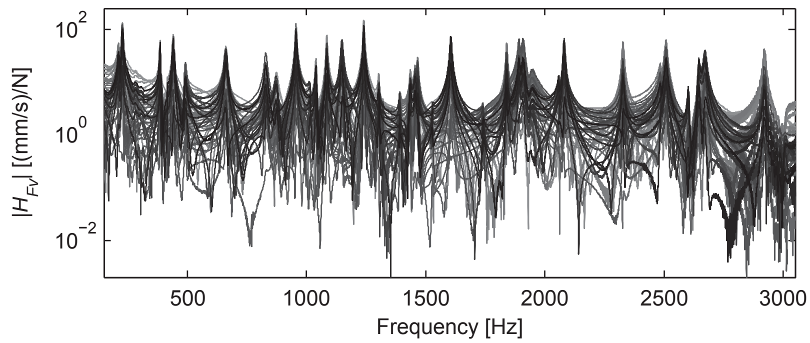

Figure 4: The magnitude of the frequency response functions for all 51 (3×17) measurement points of the pristine structure.

Table 1: Settings for the two measurements.

	first	second
excitation	sweep	single tone
frequency	150–3050Hz	1456/1455Hz, 2328/2340Hz
domain	frequency	time
averaging	10	–
sampling frequency	50kHz	1MHz
duration	2.62s	1.05s

Phase portraits measured at $(x, y) = (0.025, 0.120)$m (center of the damage, see also Figure 1 and Figure 2) of the pristine and damage structure are made for excitation frequencies of f_4, $\tilde{f}_4$, f_6 and $\tilde{f}_6$. The phase portraits, shown in Figure 5, are based on the (measured) velocity and (calculated) acceleration responses. Each trajectory represents a different excitation amplitude. The concentric circles for the pristine structure, indicate that the motion is periodic, stable in the sense of Liapunov [9] and purely harmonic. The damaged structure also shows periodic and stable motion, but the bending deformation is harmonically distorted by the skin-stiffener damage. The motion approaches nearly fundamental harmonic behavior for the lowest excitation amplitude, while the harmonic distortion increases with increasing excitation amplitude. The damage causes the motion of the skin at the damaged region to behave dynamically nonlinear for the bending modes considered. The nonlinearities mainly occur at one side of the phase portrait while the rest of the motion remains fairly linear.

The nonlinear effects observed in the phase portraits cannot yet be linked to physical mechanisms. Therefore, the orientations and timing of the displacement, velocity and acceleration signals are analyzed in detail. Three different phases are identified:

A Opening of the delamination

B Closing of the delamination

C Contact

The skin is able to move away from the stiffener at the location of the delamination

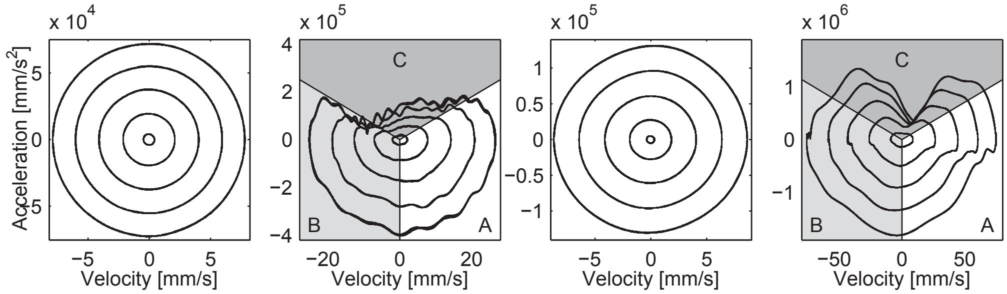

(a) (b) (c) (d)

Figure 5: Phase portraits measured at $(x, y) = (0, 025, 0.120)$m of (a,c) the pristine and (b,d) the damaged structure for a forced excitation at (a,b) the 4th bending mode ($f = 1456$Hz, $\tilde{f} = 1455$Hz) and (c,d) the 6th bending mode ($f = 2328$Hz, $\tilde{f} = 2340$Hz) and five excitation amplitude levels. The capitals refer to the opening (A), closing (B) and contact (C) phase.

for a positive difference in velocity of the skin with respect to the stiffener in z-direction (see Figure 1), causing an opening of the delamination. Similarly, a negative difference in velocity will cause the skin to move towards the stiffener, causing closing of the delamination. The velocities are equal if the skin and stiffener are in contact – though the opposite is not necessarily true. It is not possible to measure the motion of the skin and the stiffener independently in the current set-up. Therefore the motion of the stiffener is interpolated at the location of the delamination based on the motion of the skin at the points where the skin-stiffener is still intact. This approximation is justified by the large bending stiffness of the stiffener compared to that of the skin (~ 150 times).

These physical events are linked to sections in the phase portrait (Figure 5(b) and (d)) with the help of the associated displacement, velocity and acceleration waveforms for the skin at the damaged region. The skin showed a $\mathcal{O}(10\mu)$m peak-to-peak displacement at the location $(x, y) = (0.025, 0.120)$m for the highest excitation amplitude considered.

The phase portrait of the 6th bending mode shows a relatively smooth cycle compared to that of the 4th bending mode. The latter contains more high frequency components. The explanation for these difference can be found in the difference in the way the contact between skin and stiffener is (re)established. The relative difference in velocity is just one of the parameters, the location of the damage with respect to local nodes and anti-nodes of the mode shape is another parameter. The contact type can be described as either 'clapping' (with high frequency components) or 'rolling' (smooth).

4 Analytical model

An analytical model is implemented to further study the harmonic distortion induced by the damage. Initially, the objective of the model is to provide a qualitative link between the experimental observations and the hypotheses postulated on the local dynamic behaviour of the skin and stiffener at the location of the damage.

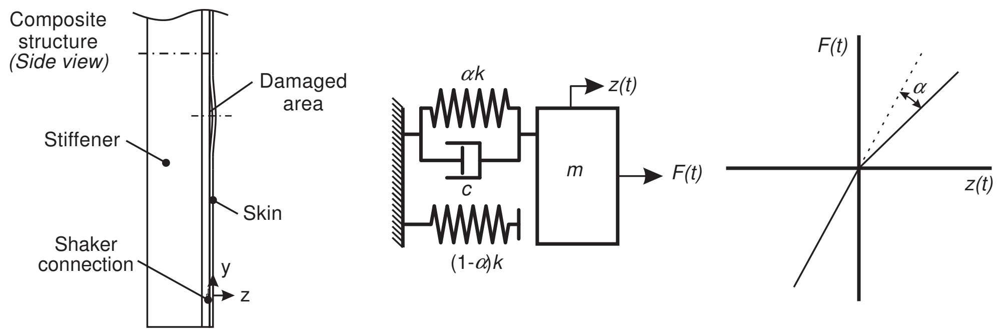

Figure 6: Delaminated skin-stiffener structure represented by a single degree of freedom bilinear mass-spring-damper system.

The dynamic behaviour of the skin-stiffener damage is represented by a mass-spring-damper system with a bilinear stiffness, depicted in Figure 6. The nonlinearity is introduced by a bilinear stiffness, representing the difference in bending stiffness for an opened delamination and a closed delamination. Note that it is assumed in this model that the motion of the stiffener is negligible compared to that of the skin. The governing dynamic equation reads:

$$\begin{array}{ll} m\,\ddot{z}(t) + c\,\dot{z}(t) + \alpha k\,z(t) = F(t) & z \geq 0 \\ m\,\ddot{z}(t) + c\,\dot{z}(t) + \quad k\,z(t) = F(t) & z < 0 \end{array} \tag{2}$$

with m the mass, c the damping, k the stiffness, α the extend of bilinearity, $z(t)$ the time-dependent displacement and $F(t)$ the (harmonic) force. The natural frequency f_n of the system can be described as a combination of the natural frequencies associated with the two stiffnesses f_k and $f_{\alpha k}$ [10]:

$$f_n = \frac{2 f_k f_{\alpha k}}{f_k + f_{\alpha k}} \tag{3}$$

The model parameters are chosen arbitrary in this first step ($m = 1$kg, $k = 10^6$N m^{-1}, $c = 50$Ns m^{-1}, $\alpha = 0.2$). The driving frequency is the natural frequency associated with the stiffness during opening of the delamination (αk; $f = 71$Hz). The normalised phase portraits are presented in Figure 7. The correspondence between the phase plot of the 4th bending mode and the analytical model is very good in qualitative sense. The correspondence with the phase portrait of the 6th bending mode is less, since the transition between the two stiffnesses is non-smooth, whereas it is expected that this is the case in reality ('rolling' contact assumption) and the assumption of a rigid stiffener is violated for this mode. It can be concluded that the model qualitatively supports the explanations given here for the experimental observations.

5 Conclusion & future prospects

The study presented here on the nonlinear dynamic behaviour of the skin and stiffener at the location of a realistic delamination damage, revealed that the interaction

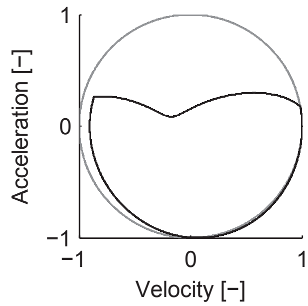

Figure 7: Analytical normalised phase portraits for a linear (gray) and bilinear (black) single degree of freedom mass-spring-damper system ($m = 1$kg, $k = 10^6$N m^{-1}, $c = 50$Ns m^{-1}, $\alpha = 0.2$).

between skin and stiffener depends on the operational deflection shape. The contact interaction ('clapping' or 'rolling') is an important parameter in the way the harmonic response of the system is distorted. The analytical model presented, qualitatively supports the explanation given for these experimental observations.

Further research will be directed towards a quantification of the experimental observation, including a parameter sensitivity study, and methods to embed the nonlinear dynamics in a structural health monitoring method.

Acknowledgements

This material is based on work supported by National Aeronautics and Space Administration, Langley Research Center under Research Cooperative Agreement No. NNL09AA00A awarded to the National Institute of Aerospace. The authors kindly acknowledge Fokker Aerostructures B.V., Hoogeveen, The Netherlands for manufacturing the composite structure used in this research. This work is funded by the European research project Clean-Sky, Eco Design ITD (grant agreement number CSJU-GAMED- 2008-001).

References

[1] A. Offringa, J. List, J. Teunissen, and H. Wiersma. Fiber reinforced thermoplastic butt joint development. In *Proceedings of International SAMPE Symposium and Exhibition*, 2008. 16 pages.

[2] C. Boller, F.K. Chang, and Y. Fujino. *Encyclopedia of Structural Health Monitoring*. John Wiley & sons, online.

[3] K. worden, C.R. Farrar, J. haywood, and M. Todd. A review of nonlinear dynamics applications to structural health monitoring. *Structural Control and Health Monitoring*, 15(4):540–567, 2008.

[4] D. Montalvao, N.M.M. Maia, and A.M.R. Ribeiro. A review of vibration-based structural health monitoring with special emphasis on composite materials. *The Shock and Vibration Digest*, 38(4):295–326, 2006.

[5] K. Diamanti and C. Soutis. Structural health monitoring techniques for aircraft composite structures. *Progress in Aerospace Systems*, 46(8):342–352, 2010.

[6] A. Raghavan and C.E.S. Cesnik. Review of guided-wave structural health monitoring. *The Shock and Vibration Digest*, 39(4):91–114, 2007.

[7] M. Richardson and B. Schwarz. Model parameter estimation from operating data. *Sound and Vibration Magazine*, page 8, January 2003.

[8] A. Klepka, W.J. Staszewski, R.B. Jenal, M. Szwedo, T.Uhl, and J. Iwaniec. Nonlinear acoustics fo fatigue crack detection - experimental investigation of vibro-acoustic wave modulations. *Structural Health Monitoring*, 11:197–211, 2012.

[9] L. Meirovitch. *Fundamentals of Vibrations*. McGraw-Hill, 1 edition, 2001. ISBN 0-07-118174-1.

[10] J. Lee. Free vibration analysis of delaminated composite beams. *Computers and Structures*, 74:121–129, 2000.